A General Strategy for Designing Two-dimensional High-efficient Layered Thermoelectric Materials

Xiwen Zhang[1], Yilv Guo[2], Zhaobo Zhou[2], Yunhai Li[2], Yunfei Chen[1]* and Jinlan Wang[1]*

[1]School of Physics & School of Mechanism Engineering, Southeast University, Nanjing 211189, China

[2]School of Physics, Southeast University, Nanjing 211189, China

Table of Contents

bulk $BiBi_2Te_2S$ at HSE+SOC level, respectively.

17. Calculated electronic band structures of 2D $BiBi_2Te_2S$ consisting of 11 atomic layers, 2D $BiBi_2Te_2S$ consisting of 22 atomic layers, and bulk $BiBi_2Te_2S$ at PBE+SOC level, respectively.

18. Calculated total energies of 2L Bi_2Se_3 and 2D $BiBi_2Se_3$ with different possible stacking models.

19. Calculated cohesive energy and binding energy of 2D $BiBi_2X_3$ (X=S/Se/Te), 2L Bi_2X_3 (X= S/Se/Te), and Bi ML, respectively.

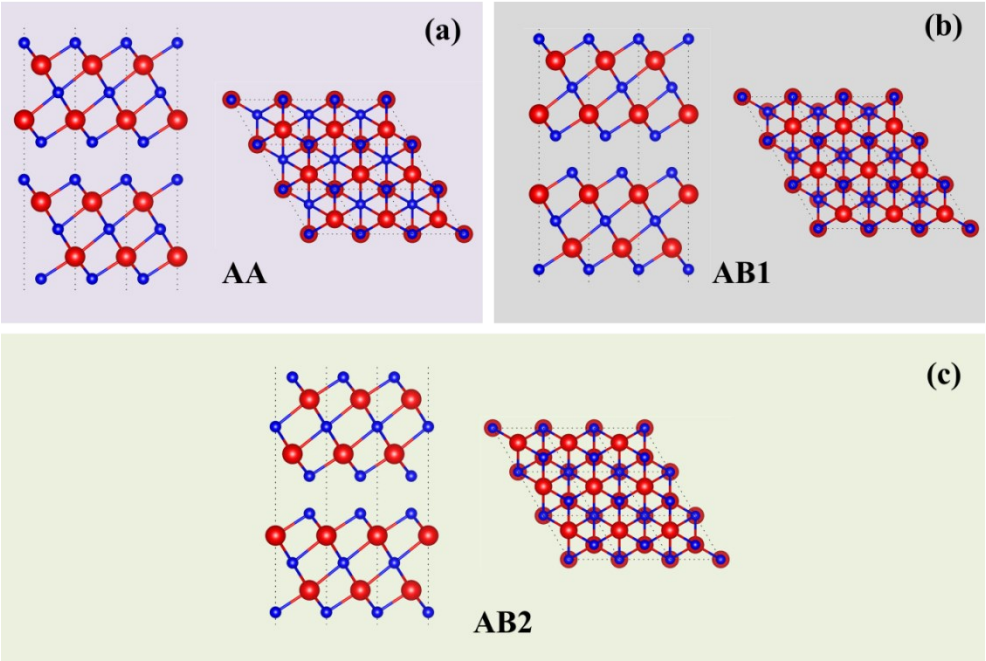

Figure S1. Side and top views of three possible stacking models (AA, AB1 and AB2) for bilayer (2L) Bi_2Se_3. Red and blue balls stand for Bi and Se atoms, respectively.

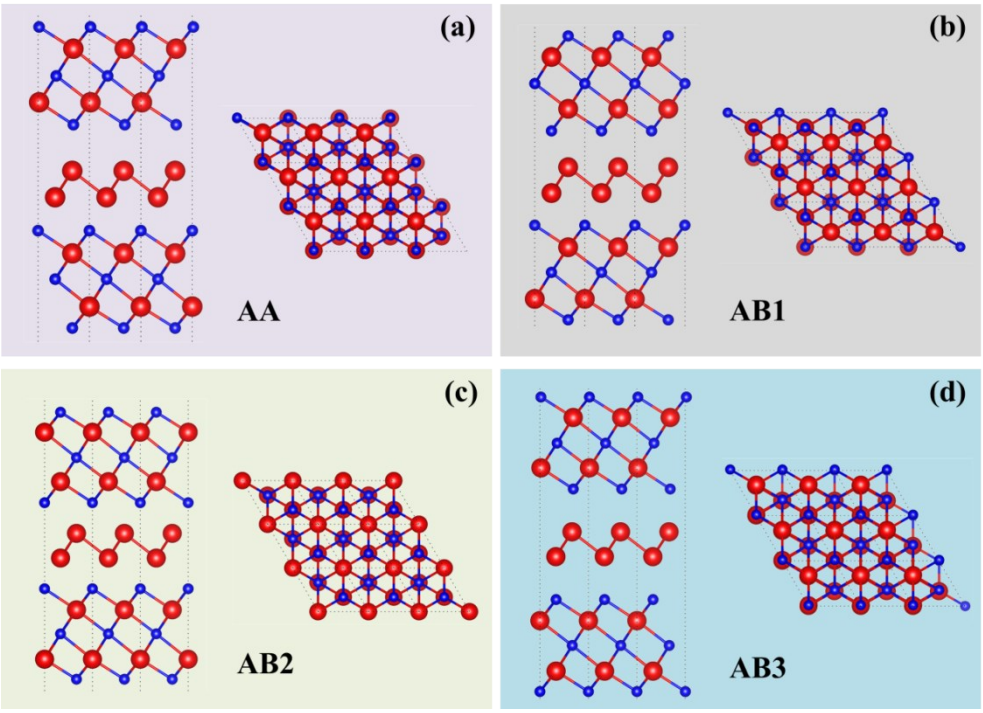

Figure S2. Side and top views of three possible stacking models (AA, AB1 and AB2) for 2D $BiBi_2Se_3$. Red and blue balls stand for Bi and Se atoms, respectively.

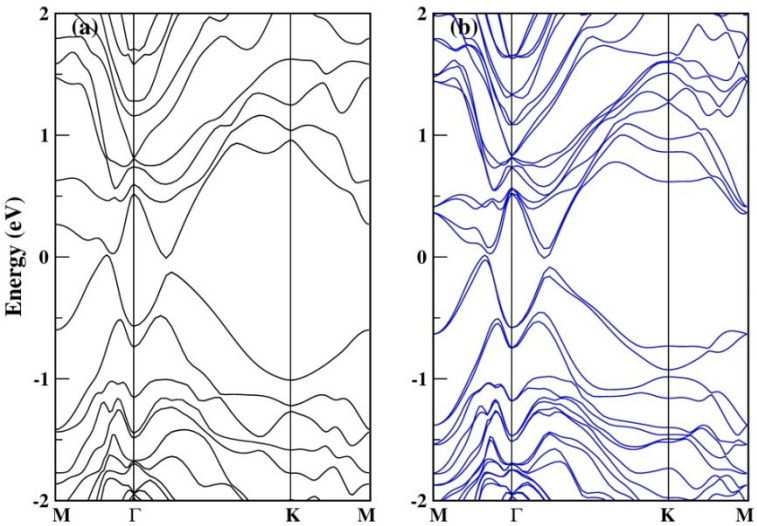

Figure S3. Calculated electronic band structures of 2D $BiBi_2Se_3$ with AB1 and AB2 stacking patterns at PBE+SOC level. The electronic band structure of 2D $BiBi_2Se_3$ with AB1 stacking pattern (two staggered Se layers) appears to be slightly non-degenerate due to the reduction of crystal symmetry.

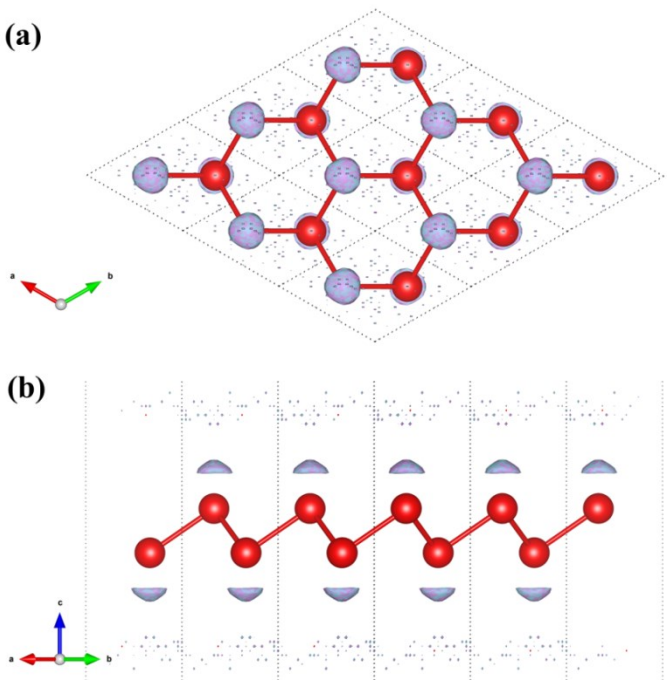

Figure S4. Electronic localization function (ELF) of Bi monolayer. Calculated ELF results show that the p_z-orbital occupied lone pairs are covering the Bi ML. The red balls represent Bi atoms. The isosurface value is set to 0.75.

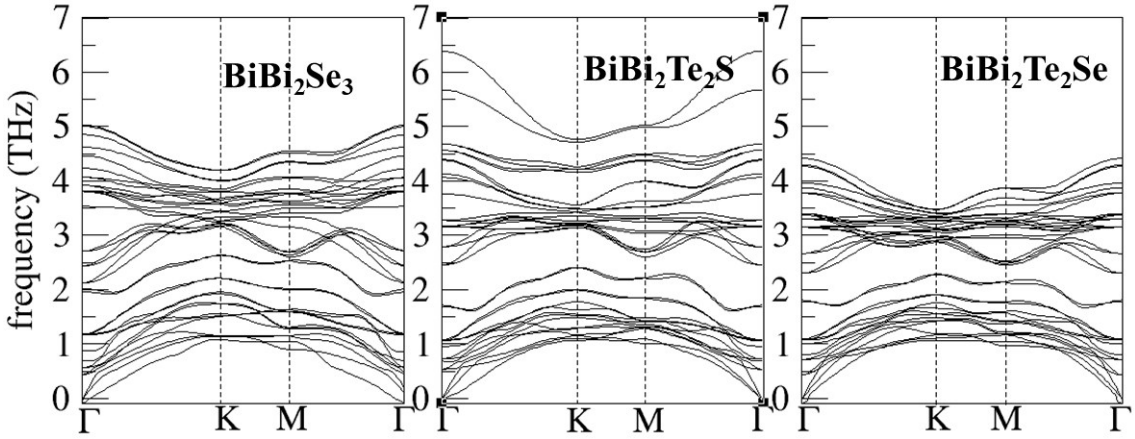

Figure S5. Phonon dispersion relations of 2D $BiBi_2X_3$ (X=S/Se/Te). There is no imaginary phonon mode appears in the whole Brillouin zone, which indicates that the 2D $BiBi_2X_3$ are dynamically stable.

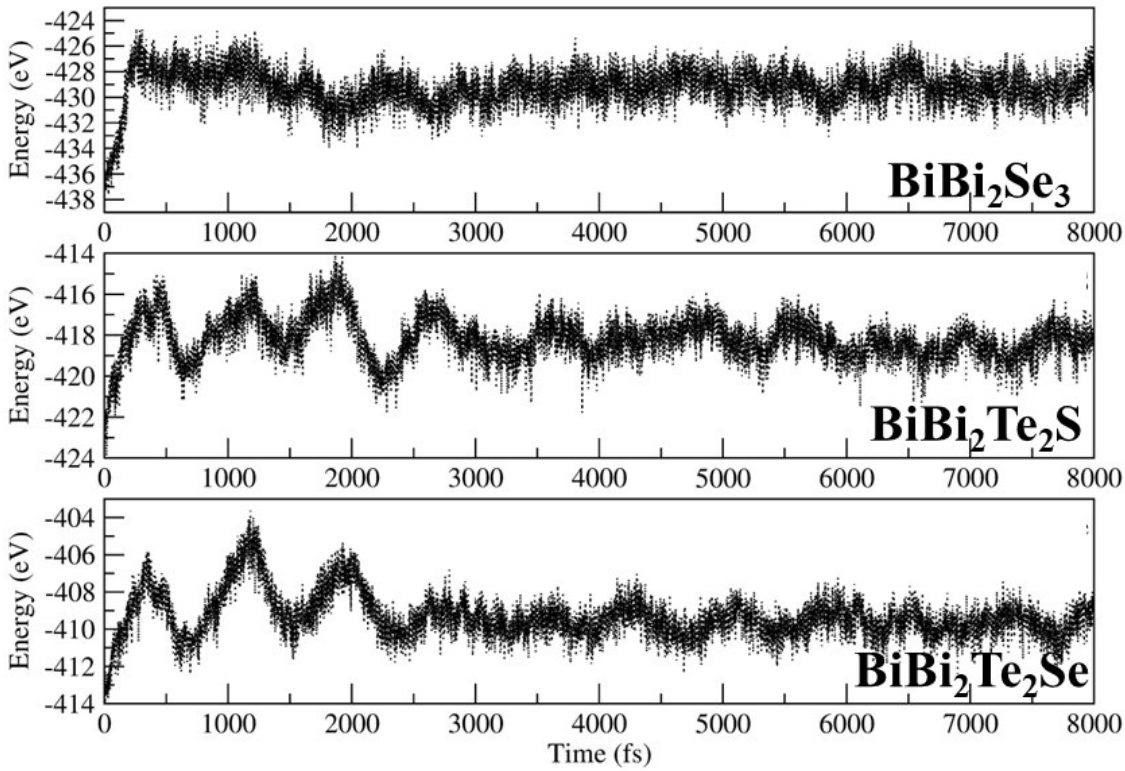

Figure S6. Variation of total energy as a function of time at 300 K. AIMD simulation in the NVT ensemble lasts for 8 ps with a time step of 2fs. The total energies of 2D $BiBi_2X_3$ (X=S/Se/Te) fluctuate around a constant value with a considerably small fluctuation magnitude.

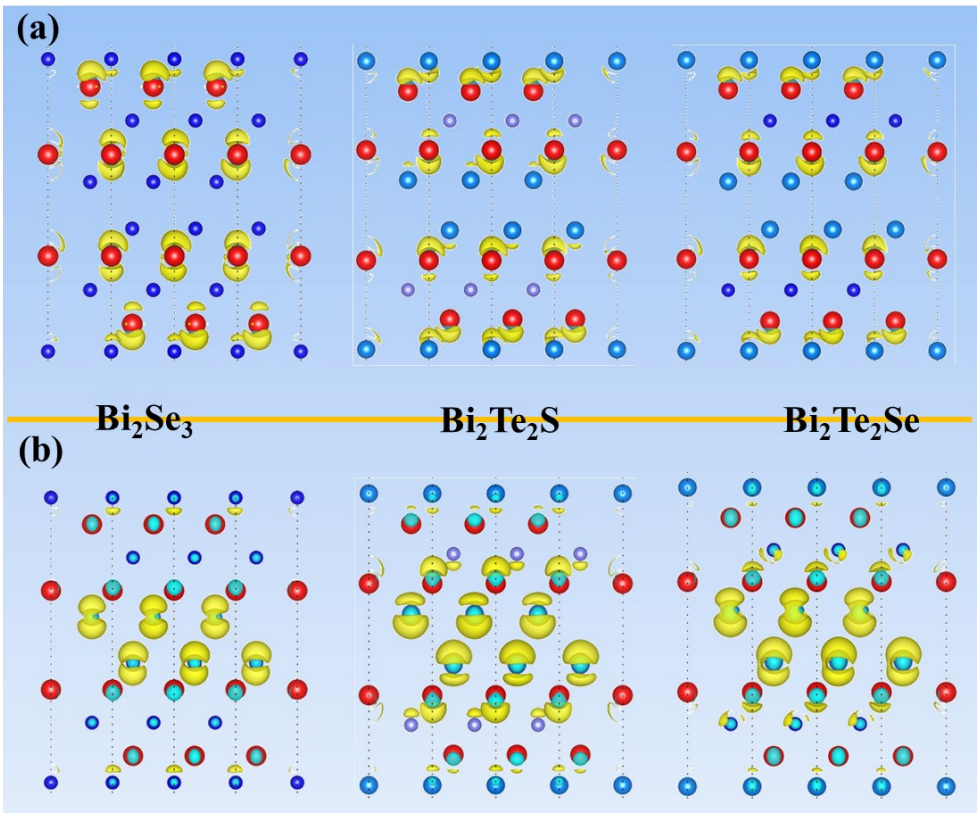

Figure S7. Calculated partial charge density of Bi_2X_3 (X=S/Se/Te) monolayers at CBM (a) and VBM (b), respectively. Red, light blue, blue, and light purple colors represent Bi, Te, Se, and S, respectively.

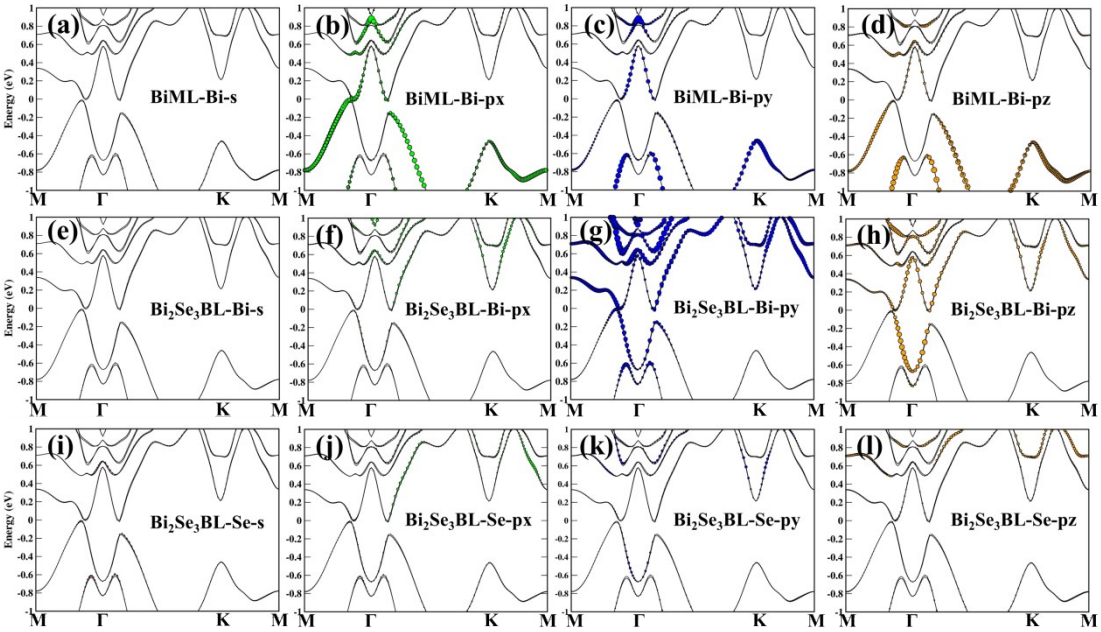

Figure S8. Calculated fat-band representation of 2D $BiBi_2Se_3$ consisting of 11 atomic layers. Red, green, blue, and orange stand for s-, px-, py-, and pz-orbital contribution, respectively.

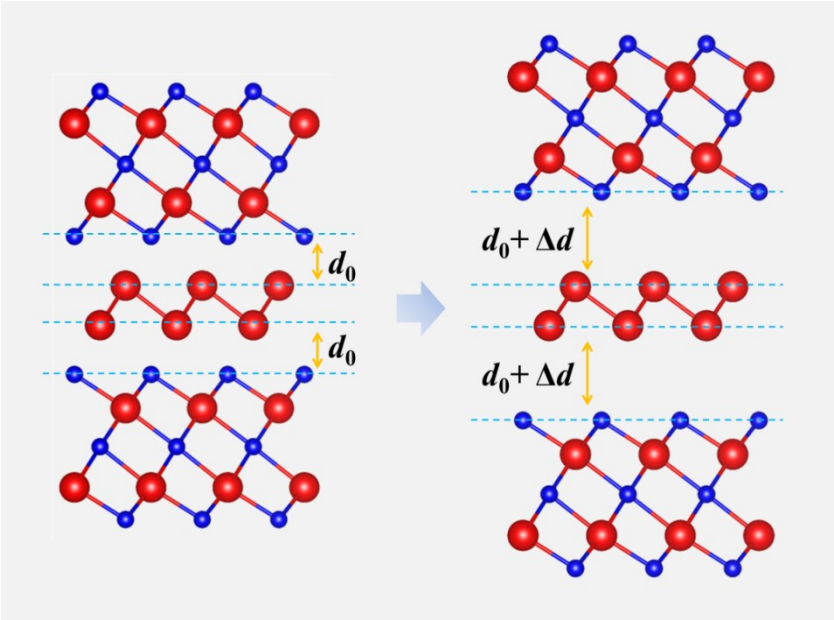

Figure S9. A schematic of decreasing the interlayer distance between the Bi ML and the two quintuplet Bi_2Se_3 layers to the stable $BiBi_2Se_3$ consisting of 11 atomic layers. d_0 and $\Delta d_{B\text{-}BS}$ represent the vdW gap of the 2D stable $BiBi_2Se_3$ and the variation of interlayer distance between the Bi ML and the two quintuplet Bi_2Se_3 layers, respectively. Red and blue balls stand for Bi and Se atoms, respectively.

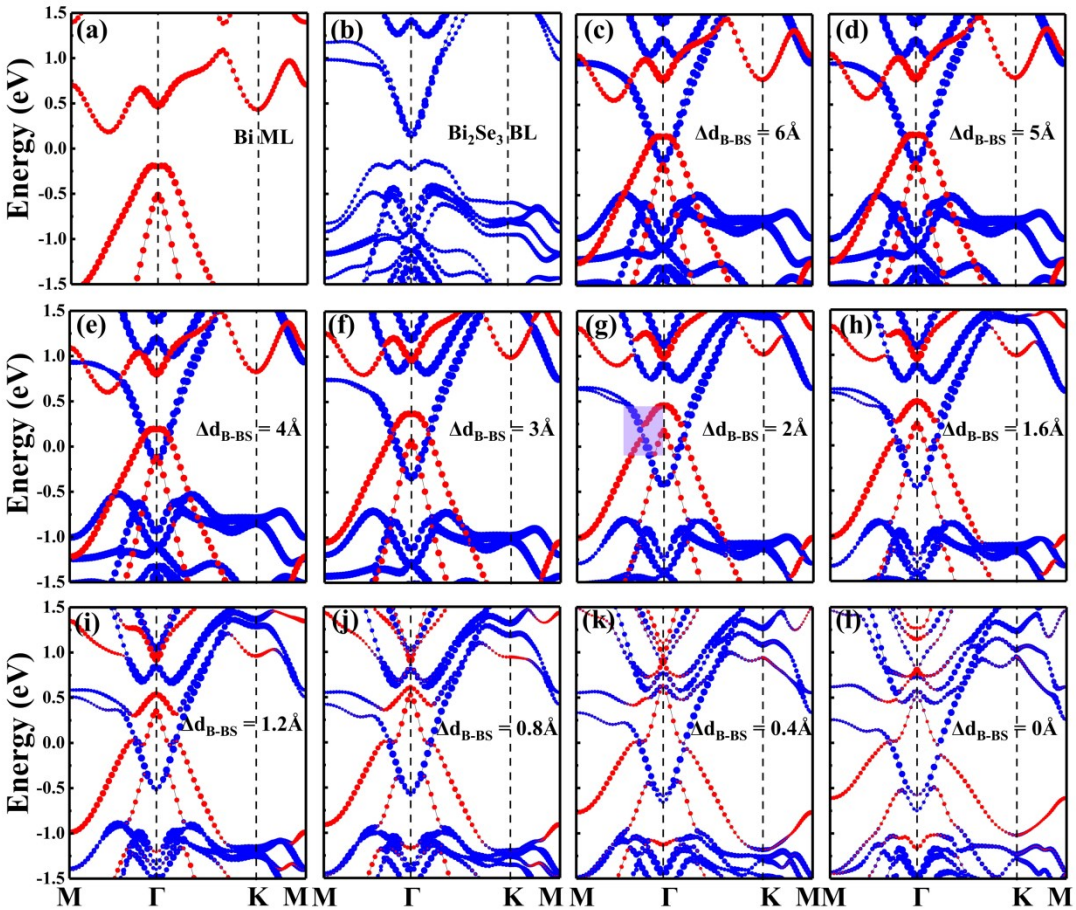

Figure S10. Calculated electronic bands of Bi ML, two quintuplet Bi_2Se_3 layers (2L) and 2D $BiBi_2Se_3$ with a series of different $\Delta d_{B\text{-}BS}$ at PBE+SOC level. The red and blue dots stand for the contribution from Bi ML and Bi_2Se_3 2L, respectively. We monotonously decrease the interlayer distance between the Bi ML and the two quintuplet Bi_2Se_3 layers, and obtain a series of corresponding electronic band structures, as shown in Fig. 3. We noticed from Fig. 3 that both Bi ML and two quintuplet Bi_2Se_3 layers maintain individual and complete electronic band structure until the variation ($\Delta d_{B\text{-}BS}$) of interlayer distance is decreased to 3Å. Interestingly, the electronic band structures of Bi ML and two quintuplet Bi_2Se_3 layers start to appear an obvious hybridization at the $\Delta d_{B\text{-}BS}$ of 2Å (Fig. 3e), and this hybridization is getting stronger and stronger with the further decreasing of $\Delta d_{B\text{-}BS}$. At the Δd of 0.8Å, the reconstructed electronic band structure is formed. We think that this is an amazing electronic band structure evolving process, which is also likely to occur in other similar multilayer structures.

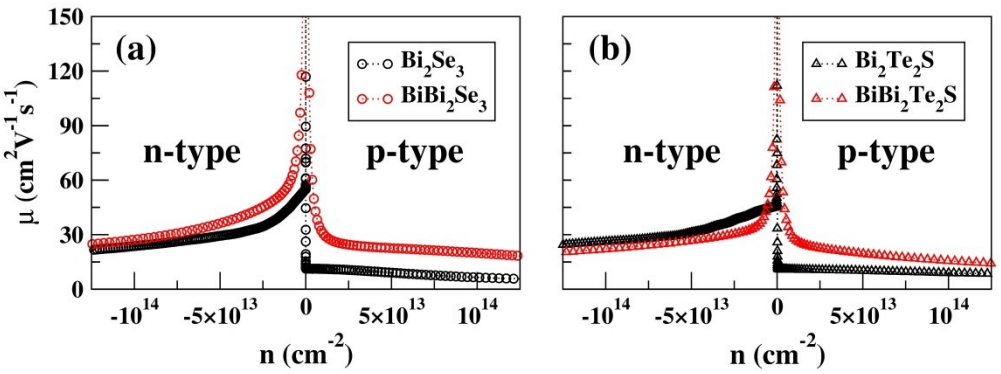

Figure S11. Calculated carrier mobility (μ) of Bi intercalated and non-intercalated 2L Bi_2Se_3 and Bi_2Te_2S.

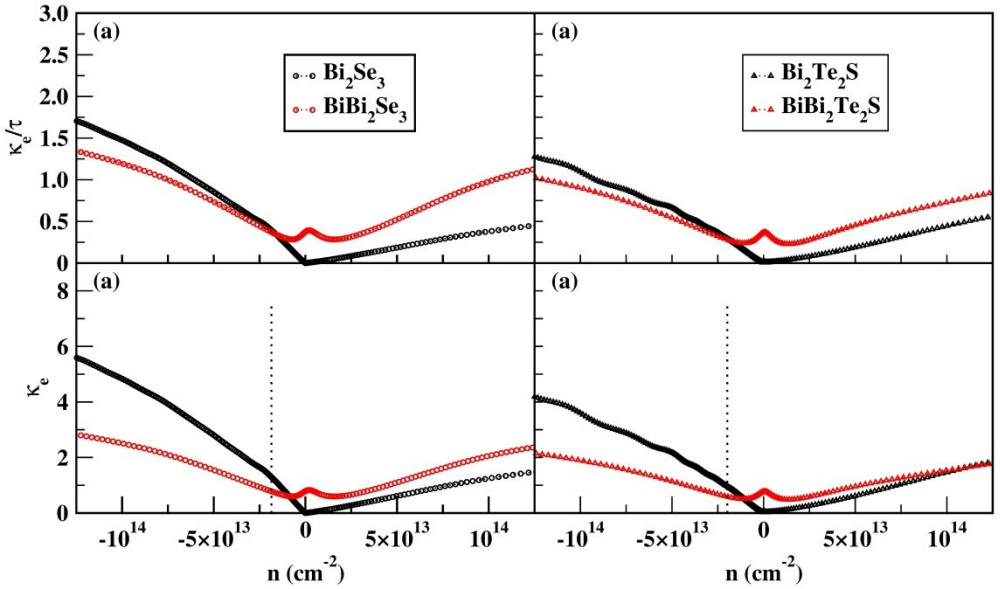

Figure S12. Calculated electronic thermal conductivity relative to relaxation time (κ_e/τ) and electronic thermal conductivity (κ_e) of 2L Bi_2Se_3/Bi_2Te_2S and 2D Bi ML inserted Bi_2Se_3/Bi_2Te_2S crystals as a as a function of carrier concentration (n) at 300 K. The units for κ_e/τ and κ_e are $Wm^{-1}K^{-1}s^{-1}$ and $Wm^{-1}K^{-1}$, respectively.

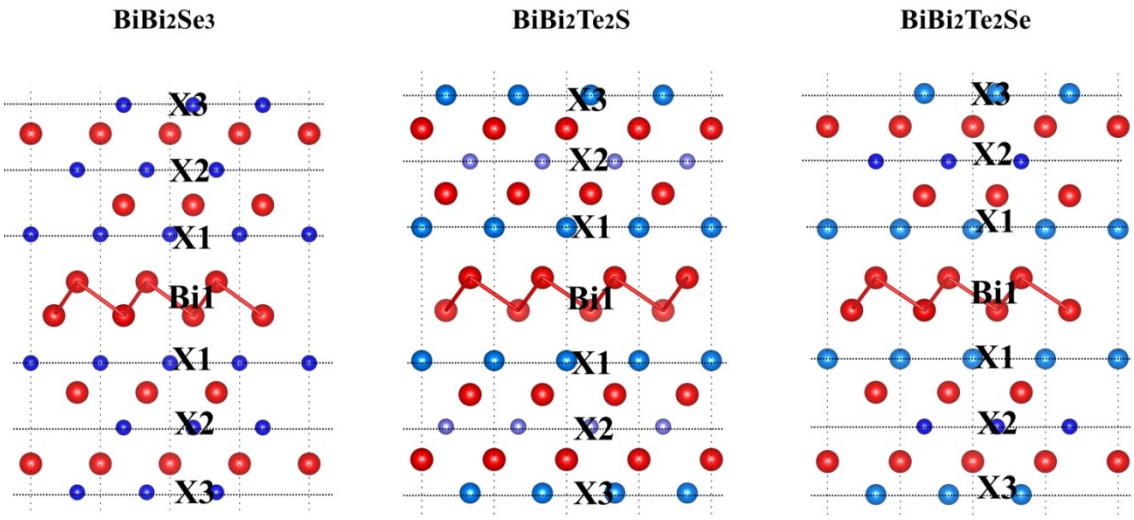

Figure S13. Position of Bi1, X1, X2, and X3 atoms in 2D Bi_3X_3 (X=S/Se/Te) crystal. Red, light blue, blue, and light purple colors represent Bi, Te, Se, and S, respectively.

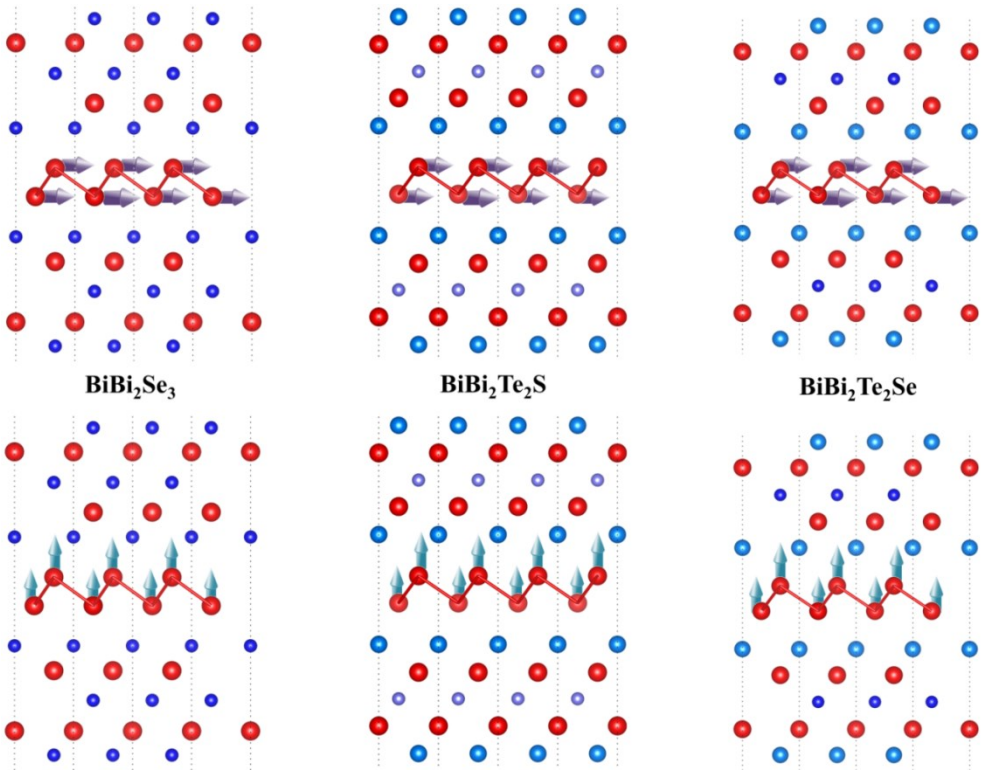

Figure S14. Normal modes with localized vibrations of Bi middle bilayer in $BiBi_2X_3$ (X=S/Se/Te) in the low-frequency A-region (marked in pink color in Fig. 5a). Red, light blue, blue, and light purple colors represent Bi, Te, Se, and S, respectively.

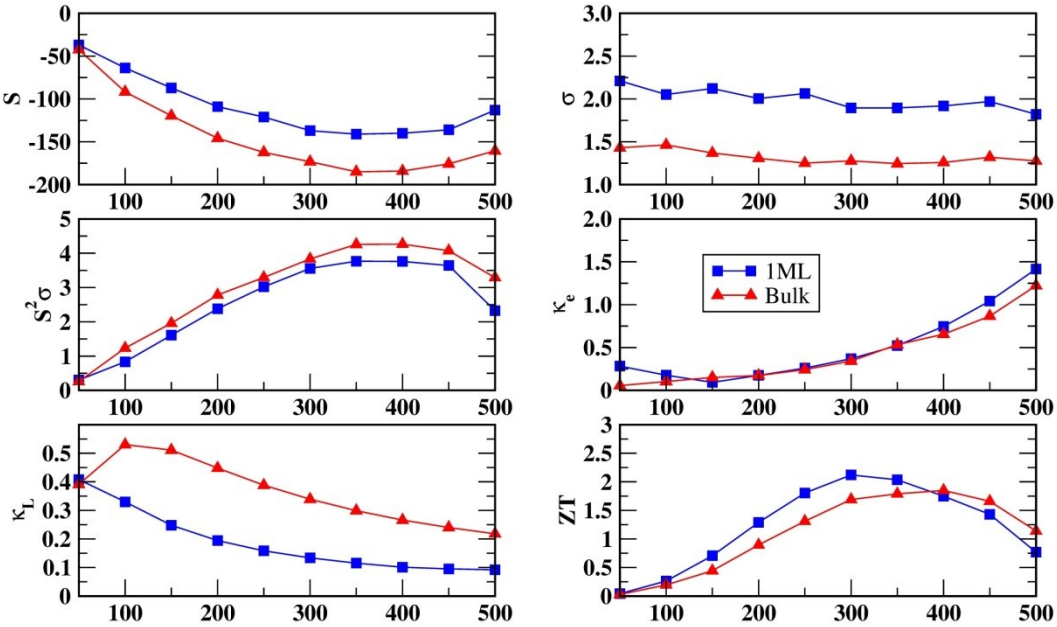

Figure S15. Calculated thermoelectric (TE) properties of 2D $BiBi_2Te_2S$ consisting of 11 atomic layers (1L) and bulk $BiBi_2Te_2S$ at the optimum concentration (n) where the maximum PF occurs in n-dependent PF, respectively. The units for S, σ, $S^2\sigma$, κ_e, and κ_L are $\mu V^{-1}K^{-1}$, $10^5\Omega^{-1}m^{-1}$, $10^{-3}Wm^{-1}K^{-2}$, $Wm^{-1}K^{-1}$, and $Wm^{-1}K^{-1}$, respectively.

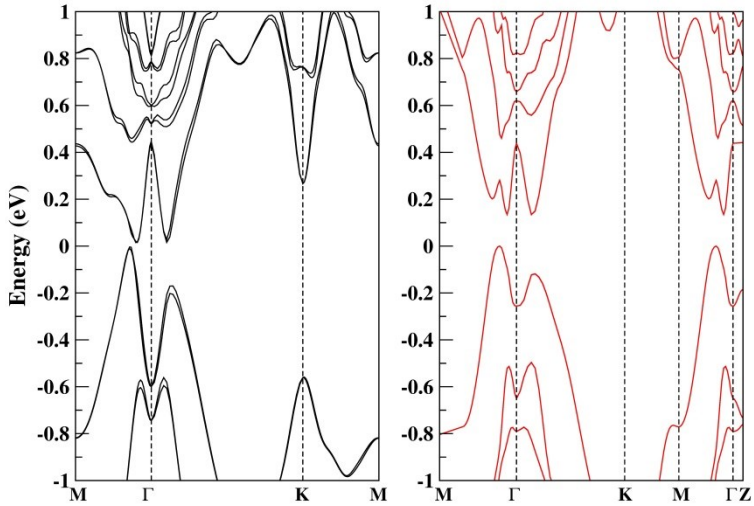

Figure S16. Calculated electronic band structures of 2D $BiBi_2Te_2S$ consisting of 11 atomic layers (1L) and bulk $BiBi_2Te_2S$ at HSE+SOC level, respectively.

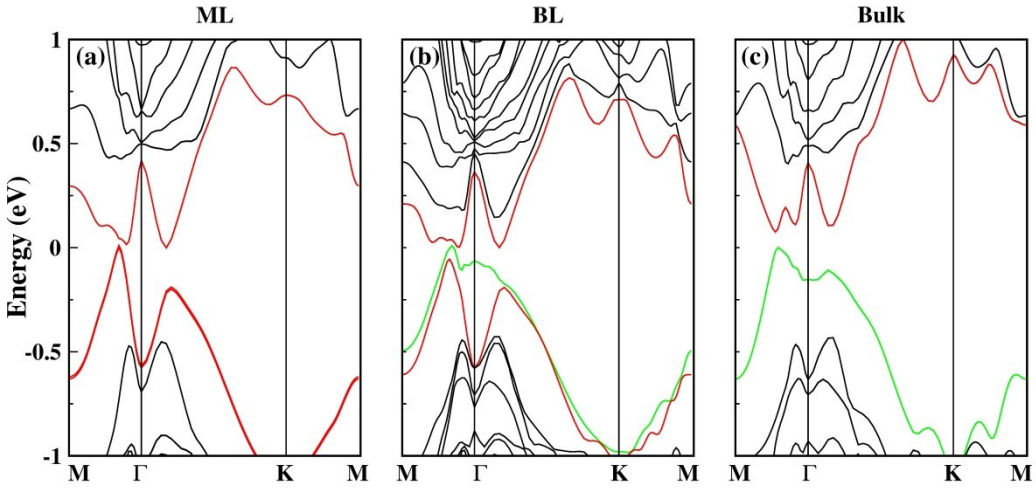

Figure S17. Calculated electronic band structures of (a) 2D $BiBi_2Te_2S$ consisting of 11 atomic layers (1L), 2D $BiBi_2Te_2S$ consisting of 22 atomic layers (2L), and (c) bulk $BiBi_2Te_2S$ at PBE+SOC level, respectively.

Table S1 Calculated total energies (units in eV) of 2L Bi_2Se_3 and 2D $BiBi_2Se_3$ with different possible stacking models.

Stacking models	**AA**	**AB1**	**AB2**	**AB3**
2L Bi_2Se_3	-46.658	**-46.711**	**-46.282**	--
2D $BiBi_2Se_3$	-57.034	**-57.179**	**-57.289**	-56.778

Cohesive energy calculation

The cohesive energy (E_{coh}) of 2D $BiBi_2X_3$ (X=S/Se/Te), 2L Bi_2X_3 (X= S/Se/Te), and Bi monolayer (ML) can be calculated by

$$E_{coh}(A_xB_y) = \frac{1}{x+y}\left(xE_{atom}^{A} + yE_{atom}^{B} - E_{tot}\right), \quad (1)$$

where x and y are the number of A and B atom in unit cell, respectively, and E_{atom}^{A}, E_{atom}^{B}, and E_{tot}, are the total energies of A atom, B atom, and 2D A_xB_y unit cell, respectively. The calculated cohesive energies of 2D $BiBi_2X_3$ (X=S/Se/Te), 2L Bi_2X_3 (X= S/Se/Te), and Bi ML are listed in Table S2.

Binding energy calculation

In order to further access the possibility to synthesize these multilayer structures, we have calculated the binding energy (E_b) of 2D $BiBi_2X_3$ (X=S/Se/Te) and 2L Bi_2X_3 via the formula:

$$E_b = E_A + E_B - E_t, \quad (2)$$

where E_A and E_B are total energies of 2D components forming the multilayer structures, and E_t is the total energy of multilayer structures.

Table S2 Calculated cohesive energy (E_{coh}) of 2D $BiBi_2X_3$ (X=S/Se/Te), 2L Bi_2X_3 (X= S/Se/Te), and Bi ML, respectively. Calculated binding energy (E_b) of 2D $BiBi_2X_3$ (X=S/Se/Te) and 2L Bi_2X_3 (X= S/Se/Te), respectively. The units are eV for both E_{coh} and E_b.

Systems	**$BiBi_2Se_3$**	**$BiBi_2Te_2S$**	**$BiBi_2Te_2Se$**	**Bi_2Se_3**	**Bi_2Te_2S**	**Bi_2Te_2Se**	**Bi**

E_{coh}	2.947	2.382	2.240	2.887	2.771	2.673	1.939
E_b	2.605	2.675	2.642	2.219	2.293	2.420	--